Acta Crystallographica Section F
Structural Biology and Crystallization Communications
ISSN 1744-3091

Refolding, purification and crystallization of the FrpB outer membrane iron transporter from *Neisseria meningitidis*

Muhammad Saleem,[a] Stephen M. Prince,[b] Hema Patel,[c] Hannah Chan,[c] Ian M. Feavers[c] and Jeremy P. Derrick[a]*

[a]Michael Smith Building, Faculty of Life Sciences, University of Manchester, Oxford Road, Manchester, England, [b]Manchester Interdisciplinary Biocentre, Faculty of Life Sciences, University of Manchester, Princess Street, Manchester, England, and [c]National Institute for Biological Standards and Control, Health Protection Agency, Blanche Lane, South Mimms, Potters Bar, Hertfordshire, England

Correspondence e-mail: jeremy.derrick@manchester.ac.uk

Received 2 December 2011
Accepted 28 December 2011

FrpB is an integral outer membrane protein from the human pathogen *Neisseria meningitidis*. It is a member of the TonB-dependent transporter family and promotes the uptake of iron across the outer membrane. There is also evidence that FrpB is an antigen and hence a potential component of a vaccine against meningococcal meningitis. FrpB incorporating a polyhistidine tag was over-expressed in *Escherichia coli* into inclusion bodies. The protein was then solubilized in urea, refolded and purified to homogeneity. Two separate antigenic variants of FrpB were crystallized by sitting-drop vapour diffusion. Crystals of the F5-1 variant diffracted to 2.4 Å resolution and belonged to space group *C*2, with unit-cell parameters a = 176.5, b = 79.4, c = 75.9 Å, β = 98.3°. Crystal-packing calculations suggested the presence of a monomer in the asymmetric unit. Crystals of the F3-3 variant also diffracted to 2.4 Å resolution and belonged to space group $P2_12_12_1$, with unit-cell parameters a = 85.3, b = 104.6, c = 269.1 Å. Preliminary analysis suggested the presence of an FrpB trimer in the asymmetric unit.

1. Introduction

Neisseria meningitidis is the causative agent of meningococcal meningitis and septicaemia. It constitutes a serious public health problem in both the developed and the developing world. The bacterium expresses several different serogroups defined by the nature of the surface capsular polysaccharide (Feavers & Pizza, 2009). The introduction of a conjugate vaccine against serogroup C organisms has been highly effective, but disease caused by serogroup B bacteria remains a problem (Feavers & Pizza, 2009; Zollinger *et al.*, 2011). Concerns about possible cross-reaction of antibodies against the serogroup capsule with foetal antigens have led to a focus on the outer membrane proteins (OMPs) of the bacterium as vaccine components. Parts of the OMP can be exposed to the external environment and hence are in principle accessible to the immune system. Several clinical trials have shown that vaccines based on outer membrane vesicles, which harbour integral OMPs, can be effective in combating the disease (Cartwright *et al.*, 1999; Feavers & Pizza, 2009). The application of such an approach is limited, however, by the antigenic variation of the major OMPs. For example, vaccines can protect against disease caused by one variant of the porin protein PorA, but are much less effective against other meningococcal isolates which harbour other PorA variants (Feavers & Pizza, 2009). Sequence variation within integral OMPs is generally concentrated into 'loop' regions, which are predicted to be surface-exposed (Urwin *et al.*, 2004). Epidemiological modelling provides a plausible explanation of the diversity of OMP antigenic variants within a population based on the principle of immune selection (Gupta *et al.*, 1996). The current view is therefore that particular OMP antigenic variants arise and proliferate within a population and that this process is driven by immune selection.

FrpB is an integral OMP and is predicted on the basis of sequence similarity to belong to the family of TonB-dependent transporters (TBDTs; Pettersson *et al.*, 1995; Beucher & Sparling, 1995). TBDTs are widespread in Gram-negative bacteria and the crystal structures of several have been determined (Krewulak & Vogel, 2008). A

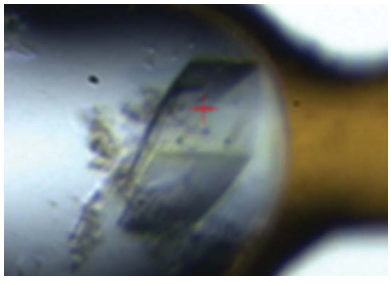

prototypical TBDT structure consists of a 22-stranded antiparallel β-barrel with an N-terminal α/β 'plug' domain which packs into the barrel interior. TBDTs are responsible for the uptake of a variety of substrates across the outer membrane, including iron–siderophore complexes, haem and cobalamin (vitamin B_{12}). In some cases additional protein components are required for substrate capture: an example is the haemophore HasA, a small protein which binds haem with high affinity and then passes it on to the TBDT HasR (Braun & Hantke, 2011; Krieg *et al.*, 2009). Several crystal structures have been determined of complexes of TBDT with transported substrates; recognition of the transported substrate occurs at the outside end of the interior surface of the barrel (Krewulak & Vogel, 2008). This initial binding event is energy-independent, but the second transport step requires interaction with the inner membrane protein TonB. Binding of TonB to a short stretch of residues at the N-terminus of the TBDT, termed the 'TonB box', initiates the transport step and is linked to the transmembrane electromotive potential across the inner membrane. The precise mechanisms of this transport step remain to be elucidated.

Expression of FrpB is known to be inducible under conditions of iron limitation (Dyer *et al.*, 1988). However, deletion of the gene does not produce a difference in iron utilization in *Neisseria meningitidis* or *N. gonorrhoeae* (Pettersson *et al.*, 1995; Beucher & Sparling, 1995). Experiments aimed at identifying the specificity of FrpB failed to provide conclusive evidence for the transport of haem, iron–citrate or iron–enterobactin (Beucher & Sparling, 1995). Similarly, transferrin and lactoferrin could not be established as sources of iron for transport by FrpB. Experiments conducted on FrpB in *N. gonorrhoeae* provided evidence for the transport of an iron–enterobactin complex, but the affinity of the transporter for the substrate was relatively low (Carson *et al.*, 1999). The question of the identity of the transported substrate of FrpB therefore remains open at present. In some publications, FrpB from *N. meningitidis* and *N. gonorrhoeae* is referred to as FetA (Carson *et al.*, 1999). It should be appreciated, however, that this protein is distinct from the TBDT FetA from *Pseudomonas fluorescens*, which binds ferric enantiopyochelin, an iron siderophore (Brillet *et al.*, 2011). For clarity and consistency, we will use the name FrpB in this manuscript.

FrpB has been shown to induce the production of bactericidal antibodies (Pettersson *et al.*, 1990; Kortekaas *et al.*, 2006) and is a candidate component of a vaccine against meningococcal disease (Urwin *et al.*, 2004). However, such antibodies are strain-specific owing to sequence variation concentrated within the segments of the protein which are exposed at the external surface (Thompson *et al.*, 2003). Sequence variants map to the external loop L5 and also, to a lesser extent, L3, with the former shielding the latter from immune recognition (Kortekaas *et al.*, 2006). The role of FrpB as a vaccine component, plus the ambiguity concerning the nature of its transported substrate, provide a strong incentive to determine its three-dimensional structure. Here, we report the crystallization and preliminary X-ray diffraction data of two FrpB antigenic variants, which paves the way for an investigation of these questions at the molecular level.

2. Materials and methods

2.1. Cloning, expression and purification

Coding sequences for the F3-3 and F5-1 loop 5 variants of FrpB were amplified from meningococcal genomic DNA and ligated at a ligation-independent cloning site (LIC) into pET30EkLIC (Novagen, Merck Biosciences). This resulted in a translated protein which replaces the predicted 22-residue signal peptide with the sequence MHHHHHHSSGLVPRGSGMKETAAAKFERQHMDSPDLGTD-DDDK incorporating an N-terminal hexahistidine tag. This is joined to the FrpB sequence, which starts at MAENNAK . . . and terminates with . . . NYKF. This gives a translated protein with a predicted molecular mass of 82 000. The sequences of the F3-3 and F5-1 variants are given in Thompson *et al.* (2003). Recombinant FrpB was expressed as inclusion bodies (IBs) in modified *Escherichia coli* strain T7 Express (New England Biolabs). Cells were grown in 2×YT medium with 50 µg ml^{-1} kanamycin at 310 K until an OD_{600} of 0.8 was reached. FrpB expression was induced by the addition of 1 m*M* isopropyl β-D-1-thiogalactopyranoside (IPTG). The cells were incubated at 310 K with shaking for a further 4 h after induction and then harvested by centrifugation at 6000*g* for 20 min at 277 K. Cells were disrupted by sonication assisted by the addition of lysozyme (5 mg per gram of cells) and DNase (35 µg per gram of cells). IBs were sedimented by centrifuging the sonication mixture at 14 000*g* for 20 min and washed once with 50 m*M* Tris–HCl pH 7.9, 1.5%(*v*/*v*)

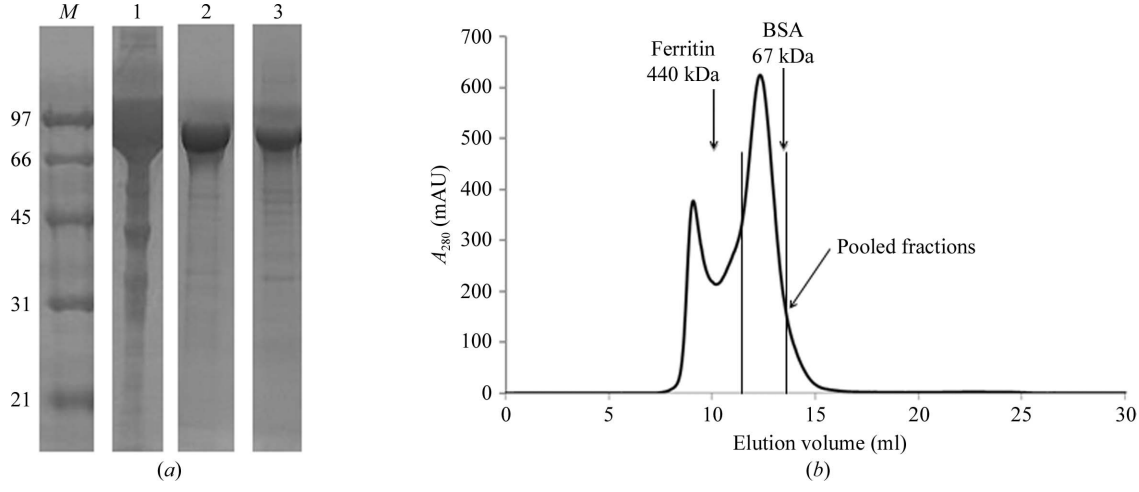

Figure 1
Purification of FrpB F3-3. (*a*) Denaturing SDS–PAGE analysis of the purification of FrpB F3-3. Lane *M*, low-range molecular-mass markers (labelled in kDa); lane 1, FrpB F3-3 after refolding and metal-chelate affinity column; lane 2, FrpB F3-3 after chromatography on Superdex 200 10/30; lane 3, FrpB F3-3 following detergent exchange (from LDAO to C_8E_5) using a metal-affinity column immediately before crystallization. (*b*) Typical elution profile of FrpB F3-3 on size-exclusion chromatography using a Superdex 200 10/30 column. The elution positions of the molecular-mass markers ferritin and BSA are indicated. Other details are as given in §2.

Table 1
Diffraction data statistics for *N. meningitidis* FrpB variants F3-3 and F5-1.

Values in parentheses are for the outer resolution shell.

Variant	F3-3	F5-1
Space group	$P2_12_12_1$	$C2$
Unit-cell parameters (Å, °)	a = 85.3, b = 104.6, c = 269.1	a = 176.5, b = 79.4, c = 75.9, β = 98.3
X-ray source (Å)	DLS† I24	DLS† I04
Wavelength (Å)	0.978	0.946
Resolution range (Å)	134–2.40 (2.46–2.40)	40–2.40 (2.46–2.40)
Multiplicity	3.8 (2.2)	2.8 (2.80)
Significance ($\langle I\rangle$/sd)	10.2 (2.3)	9.1 (1.8)
No. of unique reflections	86235	40182
Completeness (%)	90.7 (83.1)	98.5 (99.7)
$R_{\rm merge}$‡ (%)	10.8 (37.9)	9.5 (63.8)
No. of molecules per asymmetric unit	3	1
Matthews coefficient (Å^3 Da^{-1})	2.6	3.4
Solvent content (%)	53	64

† Diamond Light Source. ‡ $R_{\rm merge} = \sum_{hkl}\sum_i |I_i(hkl) - \langle I(hkl)\rangle|/\sum_{hkl}\sum_i I_i(hkl)$.

lauryldimethylamine oxide (LDAO) followed by two washes with 50 m*M* Tris–HCl pH 7.9 alone. Approximately 0.5 g wet weight of IBs was suspended in 40 ml denaturing buffer (10 m*M* Tris pH 7.5, 1 m*M* EDTA, 8 *M* urea). Impurities and insoluble material were removed by centrifugation at 14 000*g* for 20 min. FrpB was refolded by adding the resulting supernatant dropwise to an equal volume of buffer comprising 20 m*M* Tris–HCl pH 7.9, 1 *M* NaCl, 5%(*v*/*v*) LDAO with rapid stirring. The solution was stirred for a further hour and then dialyzed against two changes of 20 m*M* Tris–HCl pH 7.9, 0.5 *M* NaCl, 0.1%(*v*/*v*) LDAO for at least 6 h at 277 K. After dialysis, the FrpB solution was passed through a 0.45 µm filter and loaded onto a 5 ml bed-volume HisTrap column (GE Healthcare) pre-equilibrated in 20 m*M* Tris–HCl pH 7.9, 0.5 *M* NaCl, 0.1%(*v*/*v*) LDAO (buffer *A*). The column was then washed with ten column volumes of buffer *A* plus 40 m*M* imidazole before elution of FrpB with ten column volumes of 20 m*M* Tris–HCl pH 7.4, 0.5 *M* NaCl, 0.1% LDAO, 250 m*M* imidazole. The purification was monitored by running selected samples on SDS–PAGE (Fig. 1*a*). Imidazole was removed from the sample by fractionation on a HiTrap desalting column (GE Healthcare) in 20 m*M* Tris–HCl pH 7.4, 0.5 *M* NaCl, 0.1%(*v*/*v*) LDAO buffer at a flow rate of 5 ml min^{-1}. FrpB was concentrated to ∼10 mg ml^{-1} before application onto a Superdex 200 column (GE Healthcare) pre-equilibrated in 20 m*M* Tris–HCl pH 7.4, 0.5 *M* NaCl, 0.1%(*v*/*v*) LDAO buffer at a flow rate of 0.5 ml min^{-1}. Fractions corresponding to the second, lower molecular-mass, elution peak were pooled (Fig. 1*b*). Prior to crystallization, LDAO detergent was exchanged for pentaoxyethylene octyl ether, C_8E_5 (Bachem), by application of FrpB onto a 1 ml bed-volume HisTrap column followed by elution in four 1 ml fractions with 20 m*M* Tris–HCl pH 7.9, 0.5 *M* NaCl, 0.5%(*v*/*v*) C_8E_5, 500 m*M* imidazole. Eluted fractions were examined by SDS–PAGE and those containing high concentrations of FrpB (generally the first and second fractions) were pooled. The pooled FrpB fractions were then diluted tenfold into 20 m*M* Tris–HCl pH 7.9, 0.5 *M* NaCl, 0.5%(*v*/*v*) C_8E_5 to reduce the overall imidazole concentration to 50 m*M*. The FrpB solution was then concentrated to 12 mg ml^{-1} using an ultrafiltration concentrator with a molecular-mass cutoff value of 100 kDa prior to crystallization.

2.2. Protein crystallization, X-ray data collection and processing

Both FrpB variants were subjected to initial sparse-matrix crystallization screens comprising a total of about 1000 conditions. Sitting drops consisting of 100 nl protein solution plus 100 nl reservoir solution were formed a using Mosquito crystallization robot (TTP LabTech) in MRC plates (Molecular Dimensions) and incubated at 293 K. For the FrpB F3-3 variant, multiple crystals grew under different initial conditions and were screened for diffraction quality at a synchrotron-radiation source (Diamond, UK). The most promising crystals at this stage were derived from the Morpheus screen (Molecular Dimensions; Gorrec, 2009) and diffracted to ∼11 Å maximal resolution. These initial 'hit' conditions were then optimized: the most important parameters for improvement of diffraction quality were a reduction in the pH from 7 to 6, the inclusion of hexyl-β-D-maltoside and a reduction of the total precipitant (MPD/PEG 1000/PEG 3350) concentration from 37.5 to 35%. An orthorhombic crystal form of the FrpB F3-3 variant was grown by mixing 200 nl 12 mg ml^{-1} FrpB F3-3 with 200 nl reservoir solution consisting of 0.6%(*w*/*v*) hexyl-β-D-maltoside, 20 m*M* sodium L-glutamate, 20 m*M* D,L-alanine, 20 m*M* glycine, 20 m*M* lysine (racemic), 20 m*M* serine (racemic), 29 m*M* imidazole, 11.6%(*v*/*v*) MPD, 11.6%(*w*/*v*) PEG 1000, 11.6%(*w*/*v*) PEG 3350, 71 m*M* MES pH 6.0. For the FrpB F5-1 variant, a monoclinic crystal form was obtained by mixing 200 nl 12 mg ml^{-1} FrpB F5-1 with 200 nl reservoir solution consisting of 30 m*M* diethylene glycol, 30 m*M* triethylene glycol, 30 m*M* tetraethylene glycol, 30 m*M* pentaethylene glycol, 45 m*M* imidazole, 20%(*w*/*v*) PEG MME 550, 10%(*w*/*v*) PEG 20 000, 56 m*M* MES pH 6.5. For mounting, both the FrpB F3-3 and F5-1 variant crystals were soaked for 5 min in reservoir solution at 293 K and then flash-cooled in liquid nitrogen before data collection. Data were processed using *XDS* (Kabsch, 2010); relevant data-collection statistics are summarized in Table 1.

3. Results and discussion

All of the TBDT crystal structures reported to date have been derived from protein which had been directly expressed into the outer membrane in its native state, solubilized with detergent and subsequently purified (Krewulak & Vogel, 2008). However, it is our experience that not all TBDTs from a heterologous host express well in *E. coli*, so we adapted a protocol for refolding of FrpB from insoluble inclusion bodies (Kortekaas *et al.*, 2006) but with a number of key modifications informed by our previous work with the OpcA protein, in which dilution into a high concentration of zwitterionic detergent followed by affinity chromatography proved to be a successful route to crystallization (Prince *et al.*, 2001). We included the addition of an oligohistidine tag at the N-terminus to facilitate purification by metal-chelate affinity chromatography. In addition, we employed 5%(*v*/*v*) LDAO for refolding instead of 0.5%(*w*/*v*) *n*-dodecyl-*N*,*N*-dimethyl-1-ammonio-3-propanesulfonate (SB-12) as used by Kortekaas *et al.* A second point of difference was that our refolding protocol involved a 1:1 dilution of solubilized inclusion bodies following by dialysis, rather than the 20-fold dilution used by Kortekaas *et al.*

Two chromatographic purification steps were used: the first involved binding and elution from a metal-chelate affinity column and was followed by a size-exclusion step using a Superdex 200 column (Fig. 1*a*). We found the latter step to be critical for the preparation of a sample that gave crystals which diffracted to high resolution. Crystals could be grown from samples which omitted this step, but their diffraction quality was much poorer. A typical profile of a size-exclusion chromatogram is shown in Fig. 1(*b*). FrpB F3-3 eluted in two peaks, with the second at approximately the estimated molecular mass for a monomer (once allowance has been made for the detergent micelle). The first peak was of higher apparent mass and could originate either from oligomers or aggregates. The lower molecular-

(*a*)

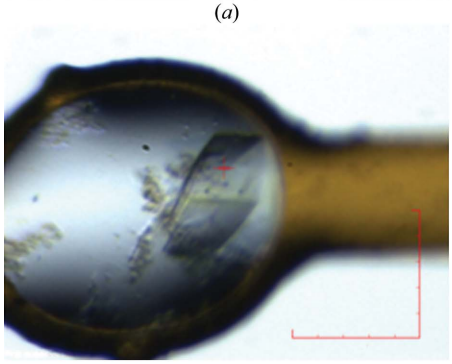

(*b*)

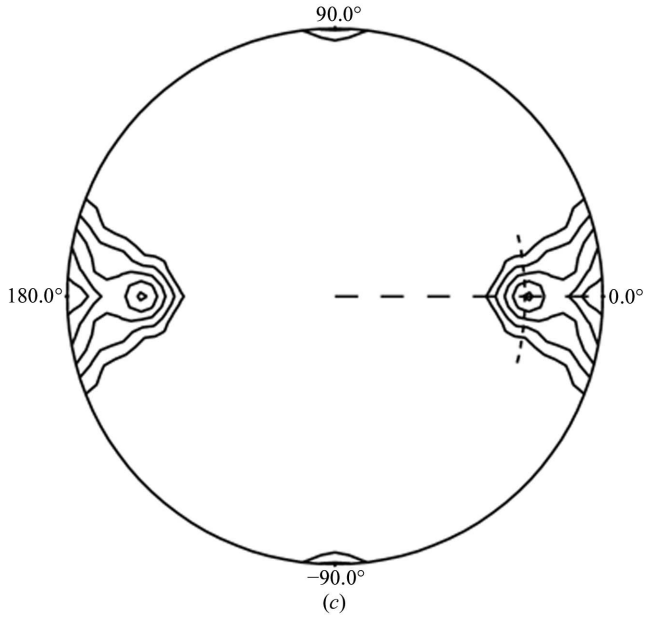

(*c*)

Figure 2
Data collection and self-rotation function. (*a*) FrpB F3-3 during data collection; the red square is 25 × 25 µm in size. (*b*) FrpB F5-1 during data collection: the axes at the bottom right are 100 µm in length. (*c*) Self-rotation function (SRF) diagram ($0 \le \omega \le 90^\circ$ $0 \le \varphi \le 360^\circ$, $\chi = 120^\circ$) determined for data from the FrpB variant F3-3 using the programs *ECALC* and *POLARRFN* from the *CCP*4 suite (Winn *et al.*, 2011). φ intervals are shown around the circumference; the coarse dotted line indicates the direction of ω and the fine dotted arc is drawn at the radius where $\omega = 71.8^\circ$. The first contour is at drawn at the root-mean-square amplitude of the SRF; successive contours are drawn at multiples of half of this value.

mass peak was routinely selected for crystallization trials. Similar results were obtained for FrpB F5-1 (not shown). Denaturing SDS–PAGE indicated a high level of purity for the final FrpB F3-3 preparation (Fig. 1*a*).

A variety of screens were used to search for suitable crystallization conditions: we obtained optimal results using the Morpheus screen (Molecular Dimensions; Gorrec, 2009). Initial screens were carried out using LDAO as a detergent, but the crystals obtained diffracted poorly. We therefore switched to the polyoxyethylene detergent C_8E_5 and obtained much better results. Detergent exchange was carried out immediately after fractionation by size exclusion and was conveniently implemented on a small metal-chelate affinity column, allowing elution of the detergent-exchanged FrpB in a small volume (Fig. 1*a*). Crystals of FrpB F3-3 took at least two weeks to grow and were up to 50 µm in the largest dimension. Data were collected on the microfocus beamline at Diamond (Fig. 2*a*), which was helpful in obtaining good-quality data (Table 1). Diffraction from the F3-3 variant was anisotropic, with some data recorded to a limit of 2.4 Å resolution but with the resolution tailing off to a maximal value of about 3.0 Å towards the end of data collection. Although it differs mainly in the sequence of the hypervariable 'loop' region, the F5-1 variant crystallized under different conditions and therefore required rescreening to optimize diffraction quality. The F5-1 variant crystals were slightly larger (Fig. 2*b*) but diffracted to a similar resolution to those of the F3-3 variant (Table 1).

Estimation of the Matthews coefficient for the F5-1 crystal form in space group *C*2 gave a value of 3.4 Å^3 Da^{-1}, assuming the presence of a monomer in the asymmetric unit. In the case of the F3-3 variant, the self-rotation function (SRF) was calculated with normalized amplitudes in the resolution interval 45–4.5 Å with a Patterson integration radius of 77 Å (corresponding to approximately half the mean unit-cell length). The SRF was expressed using spherical polar angles (Navaza, 2001) about axes *x*, *y*, *z* with *a*/*x*, *b*/*y* and *c*/*z* parallel. A peak in the constant-rotation $\chi = 120^\circ$ section at $\omega = 71.8^\circ$, $\varphi = 0/180^\circ$ indicated the presence of a noncrystallographic threefold rotation axis parallel to the *ac* plane with an angle of inclination to the *c* axis of ∼72° (Fig. 2*c*). Assuming the presence of a trimer in the asymmetric unit gives a Matthews coefficient of 2.6 Å^3 Da^{-1} (Table 1). The ability of FrpB to crystallize as a monomer or as a trimer is indicative of an equilibrium between the two quaternary states which could be influenced by crystallization conditions. Kortekaas and coworkers noted that FrpB assembles into oligomers (assumed to be dimers) and that this phenomenon was correlated with an enhanced immune response in animal vaccination trials (Kortekaas *et al.*, 2006). The presence of noncrystallographic symmetry in the FrpB F3-3 variant may therefore be relevant to these observations, suggesting that immunogenicity could be stimulated by the formation of FrpB trimers, at least for some variants.

Determination of the crystal structure of FrpB will provide some vital clues to its specificity for the transported substrate. A comparison of the structures of the F3-3 and F5-1 variants will also help to address a second but equally important question: what the structures of the hypervariable 'loop' regions are within these proteins and their degree of similarity. Current models for the origin and proliferation of such variants within the meningococcal population suggest that immune selection plays a major role in determining the survival of particular variants (Gupta *et al.*, 1996). How this selection works at the structural level remains to be investigated.

We thank Danny Axford and Katherine McAuley at the Diamond synchrotron for assistance with data collection and the Wellcome

Trust for funding work on FetA expression and refolding through a Translation Award.

References

Beucher, M. & Sparling, P. F. (1995). *J. Bacteriol.* **177**, 2041–2049.
Braun, V. & Hantke, K. (2011). *Curr. Opin. Chem. Biol.* **15**, 328–334.
Brillet, K., Reimmann, C., Mislin, G. L., Noël, S., Rognan, D., Schalk, I. J. & Cobessi, D. (2011). *J. Am. Chem. Soc.* **133**, 16503–16509.
Carson, S. D., Klebba, P. E., Newton, S. M. & Sparling, P. F. (1999). *J. Bacteriol.* **181**, 2895–2901.
Cartwright, K., Morris, R., Rümke, H., Fox, A., Borrow, R., Begg, N., Richmond, P. & Poolman, J. (1999). *Vaccine*, **17**, 2612–2619.
Dyer, D. W., West, E. P., McKenna, W., Thompson, S. A. & Sparling, P. F. (1988). *Infect. Immun.* **56**, 977–983.
Feavers, I. M. & Pizza, M. (2009). *Vaccine*, **27**, B42–B50.
Gorrec, F. (2009). *J. Appl. Cryst.* **42**, 1035–1042.
Gupta, S., Maiden, M. C. J., Feavers, I. M., Nee, S., May, R. M. & Anderson, R. M. (1996). *Nature Med.* **2**, 437–442.
Kabsch, W. (2010). *Acta Cryst.* D**66**, 125–132.
Kortekaas, J., Müller, S. A., Ringler, P., Gregorini, M., Weynants, V. E., Rutten, L., Bos, M. P. & Tommassen, J. (2006). *Microbes Infect.* **8**, 2145–2153.
Krewulak, K. D. & Vogel, H. J. (2008). *Biochim. Biophys. Acta*, **1778**, 1781–1804.
Krieg, S., Huché, F., Diederichs, K., Izadi-Pruneyre, N., Lecroisey, A., Wandersman, C., Delepelaire, P. & Welte, W. (2009). *Proc. Natl Acad. Sci. USA*, **106**, 1045–1050.
Navaza, J. (2001). *International Tables for Crystallography*, Vol. *F*, edited by M. G. Rossman & E. Arnold, pp. 269–274. Dordrecht: Kluwer Academic Publishers.
Pettersson, A., Kuipers, B., Pelzer, M., Verhagen, E., Tiesjema, R. H., Tommassen, J. & Poolman, J. T. (1990). *Infect. Immun.* **58**, 3036–3041.
Pettersson, A., Maas, A., van Wassenaar, D., van der Ley, P. & Tommassen, J. (1995). *Infect. Immun.* **63**, 4181–4184.
Prince, S. M., Feron, C., Janssens, D., Lobet, Y., Achtman, M., Kusecek, B., Bullough, P. A. & Derrick, J. P. (2001). *Acta Cryst.* D**57**, 1164–1166.
Thompson, E. A. L., Feavers, I. M. & Maiden, M. C. J. (2003). *Microbiology*, **149**, 1849–1858.
Urwin, R., Russell, J. E., Thompson, E. A. L., Holmes, E. C., Feavers, I. M. & Maiden, M. C. J. (2004). *Infect. Immun.* **72**, 5955–5962.
Winn, M. D. *et al.* (2011). *Acta Cryst.* D**67**, 235–242.
Zollinger, W. D., Poolman, J. T. & Maiden, M. C. J. (2011). *Expert Rev. Vaccines*, **10**, 559–561.